

Proton-Promoted Oxygen Atom Transfer vs Proton-Coupled Electron Transfer of a Non-Heme Iron(IV)-Oxo Complex

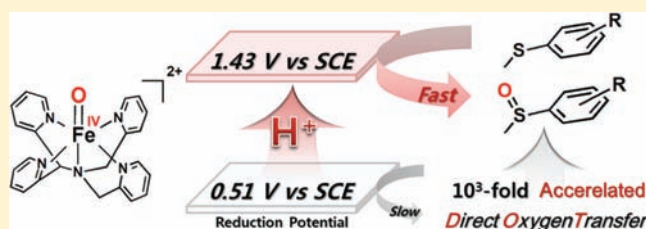
Jiyun Park,[†] Yuma Morimoto,[‡] Yong-Min Lee,[†] Wonwoo Nam,^{*,†} and Shunichi Fukuzumi^{*,†,‡}

[†]Department of Bioinspired Science, Ewha Womans University, Seoul 120-750, Korea

[‡]Department of Material and Life Science, Graduate School of Engineering, Osaka University, ALCA, Japan Science and Technology Agency (JST), Suita, Osaka 565-0871, Japan

Supporting Information

ABSTRACT: Sulfoxidation of thioanisoles by a non-heme iron(IV)-oxo complex, $[(N4Py)Fe^{IV}(O)]^{2+}$ ($N4Py = N,N$ -bis(2-pyridylmethyl)- N -bis(2-pyridyl)methylamine), was remarkably enhanced by perchloric acid (70% $HClO_4$). The observed second-order rate constant (k_{obs}) of sulfoxidation of thioanisoles by $[(N4Py)Fe^{IV}(O)]^{2+}$ increases linearly with increasing concentration of $HClO_4$ (70%) in acetonitrile (MeCN) at 298 K. In contrast to sulfoxidation of thioanisoles by $[(N4Py)Fe^{IV}(O)]^{2+}$, the observed second-order rate constant (k_{et}) of electron transfer from one-electron reductants such as $[Fe^{II}(Me_2bpy)_3]^{2+}$ ($Me_2bpy = 4,4$ -dimethyl-2,2'-bipyridine) to $[(N4Py)Fe^{IV}(O)]^{2+}$ increases with increasing concentration of $HClO_4$, exhibiting second-order dependence on $HClO_4$ concentration. This indicates that the proton-coupled electron transfer (PCET) involves two protons associated with electron transfer from $[Fe^{II}(Me_2bpy)_3]^{2+}$ to $[(N4Py)Fe^{IV}(O)]^{2+}$ to yield $[Fe^{III}(Me_2bpy)_3]^{3+}$ and $[(N4Py)Fe^{III}(OH_2)]^{3+}$. The one-electron reduction potential (E_{red}) of $[(N4Py)Fe^{IV}(O)]^{2+}$ in the presence of 10 mM $HClO_4$ (70%) in MeCN is determined to be 1.43 V vs SCE. A plot of E_{red} vs $\log[HClO_4]$ also indicates involvement of two protons in the PCET reduction of $[(N4Py)Fe^{IV}(O)]^{2+}$. The PCET driving force dependence of $\log k_{et}$ is fitted in light of the Marcus theory of outer-sphere electron transfer to afford the reorganization of PCET ($\lambda = 2.74$ eV). The comparison of the k_{obs} values of acid-promoted sulfoxidation of thioanisoles by $[(N4Py)Fe^{IV}(O)]^{2+}$ with the k_{et} values of PCET from one-electron reductants to $[(N4Py)Fe^{IV}(O)]^{2+}$ at the same PCET driving force reveals that the acid-promoted sulfoxidation proceeds by one-step oxygen atom transfer from $[(N4Py)Fe^{IV}(O)]^{2+}$ to thioanisoles rather than outer-sphere PCET.



INTRODUCTION

Brønsted acid is well-known to enhance the electrophilicity of electrophiles by interaction, making them possible to react with nucleophiles, which would otherwise exhibit no reactivity.^{1–3} Metal ion salts, which act as Lewis acids, are also known to enhance the electrophilicity of electrophiles by interacting with Lewis acids to facilitate the reactions with nucleophiles.^{4–9} The promoting effects of Brønsted acid and Lewis acids result from the activation of the C=X bond (X = O, NR, CR₂), thereby decreasing the LUMO energy and promoting the reactions with nucleophiles.^{1–9} On the other hand, both Brønsted acid and metal ions acting as Lewis acids promote electron-transfer reactions from various electron donors to electron acceptors provided that the one-electron reduced species of electron acceptors can bind with Brønsted acid (protonation) and Lewis acids, respectively. The former is classified as proton-coupled electron transfer (PCET),^{10–14} whereas the latter is regarded as metal ion-promoted electron transfer.^{15–24} It should be noted that the term of PCET has also been used for the case when an electron and a proton are transferred from the same molecule.^{25–28}

Not only the C=O bond but also the M=O (M = metal) bond can be activated by Brønsted acid and Lewis acids. In this context, we have recently reported the first example of binding

of metal ions, such as Sc^{3+} and Ca^{2+} , to a non-heme iron(IV)-oxo complex, $[(TMC)Fe^{IV}(O)]^{2+}$ ($TMC = 1,4,8,11$ -tetramethyl-1,4,8,11-tetraazacyclotetradecane), and the crystal structure of Sc^{3+} -bound $[(TMC)Fe^{IV}(O)]^{2+}$ was successfully determined by X-ray crystallography.²⁹ The binding of Sc^{3+} to $[(TMC)Fe^{IV}(O)]^{2+}$ resulted in change in the number of electrons transferred from ferrocene (Fc) to $[(TMC)Fe^{IV}(O)]^{2+}$ from one electron in the absence of Sc^{3+} to two electrons in the presence of Sc^{3+} .²⁹ Rates of electron transfer from a series of one-electron reductants to an iron(IV)-oxo complex, $[(N4Py)Fe^{IV}(O)]^{2+}$ ($N4Py: N,N$ -bis(2-pyridylmethyl)- N -bis(2-pyridyl)methylamine), were enhanced as much as 10⁸-fold in the presence of metal ions, such as Sc^{3+} , Zn^{2+} , Mg^{2+} , and Ca^{2+} , as compared with the rates in the absence of metal ion.³⁰ The rate enhancement by metal ions exhibits a good correlation with the Lewis acidity of metal ions.³⁰ The one-electron reduction potential of $[(N4Py)Fe^{IV}(O)]^{2+}$ has been demonstrated to be shifted to a positive direction by as large as 0.84 V in the presence of Sc^{3+} ion.^{30–32}

In contrast to the extensive studies on Brønsted acid-promoted reactions of organic electrophiles containing C=O bonds,^{1–9}

Received: December 27, 2011

Published: February 16, 2012

there have been only a few reports on Brønsted acid-promoted reactions of metal–oxo ($M=O$) complexes.³³ In particular, the fundamental properties of high-valent metal-oxo complexes such as the one-electron reduction potentials and the reorganization energies in PCET have yet to be reported. In addition, the relation between Brønsted acid-promoted reactions of high-valent metal-oxo complexes with nucleophiles and the PCET with one-electron reductants has yet to be clarified.

We report herein Brønsted acid-promoted oxygen atom transfer from a non-heme iron(IV)-oxo complex, $[(N4Py)Fe^{IV}(O)]^{2+}$, to thioanisoles³⁴ in comparison with PCET from one-electron reductants to $[(N4Py)Fe^{IV}(O)]^{2+}$. The PCET rate constants were evaluated in light of the Marcus theory of outer-sphere electron transfer^{35,36} to determine the one-electron reduction potential and the reorganization energy of PCET reactions of $[(N4Py)Fe^{IV}(O)]^{2+}$ in the presence of perchloric acid ($HClO_4$, 70 wt % in H_2O) in acetonitrile (MeCN). The detailed kinetic analyses on both acid-promoted oxygen atom transfer from $[(N4Py)Fe^{IV}(O)]^{2+}$ to thioanisoles and the PCET reactions from one-electron reductants to $[(N4Py)Fe^{IV}(O)]^{2+}$ provide valuable insight into the important mechanistic difference between direct oxygen atom-transfer³⁷ and outer-sphere PCET pathways, both of which are enhanced by Brønsted acid.

EXPERIMENTAL SECTION

Materials. All chemicals, which were the best available purity, were purchased from Aldrich Chemical Co. and used without further purification unless otherwise noted. Solvents, such as acetonitrile (MeCN) and diethyl ether, were dried according to the literature procedures and distilled under Ar prior to use.³⁸ Iodosylbenzene (PhIO) was prepared by a literature method.³⁹ Non-heme iron(II) complex $[(N4Py)Fe^{II}(MeCN)](ClO_4)_2$ and its iron(IV)-oxo $[(N4Py)Fe^{IV}(O)]^{2+}$ were prepared by the literature methods.³⁴ Perchloric acid (70 wt % in H_2O) was purchased from Wako Pure Chemical Ind. Ltd.

Caution: Perchlorate salts are potentially explosive and should be handled with care.

Kinetic Studies and Product Analyses. Kinetic measurements were performed on a UNISOKU RSP-601 stopped-flow spectrometer equipped with a MOS-type highly sensitive photodiode array or a Hewlett-Packard 8453 photodiode-array spectrophotometer using a 10 mm quartz cuvette (10 mm path length) at 298 K. Sulfoxidation reactions of thioanisole and its *para*-substituted derivatives (2.5×10^{-3} to 1.0×10^{-2} M) by $[(N4Py)Fe^{IV}(O)]^{2+}$ (2.5×10^{-4} M) were carried out and the rates were monitored by the decay of the absorption band at 695 nm due to $[(N4Py)Fe^{IV}(O)]^{2+}$ in the absence and presence of $HClO_4$ in MeCN at 298 K. The concentration of thioanisole derivatives was maintained at least more than 10-fold excess of $[(N4Py)Fe^{IV}(O)]^{2+}$ to attain pseudo-first-order conditions. First-order fitting of the kinetic data allowed us to determine the pseudo-first-order rate constants. The first-order plots were linear for three or more half-lives with the correlation coefficient $\rho > 0.999$. In each case, it was confirmed that the rate constants derived from at least five independent measurements agreed within an experimental error of $\pm 5\%$. The pseudo-first-order rate constants increased proportionally with an increase in concentrations of substrates, from which second-order rate constants were determined.

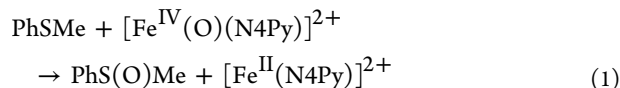
Typically, thioanisole (1.0×10^{-2} M) was added to an MeCN solution (0.50 mL) containing $[(N4Py)Fe^{IV}(O)]^{2+}$ (1.0×10^{-3} M) in the absence and presence of $HClO_4$ (1.0×10^{-2} M) in a vial. The reaction was complete within 1 h under these conditions. Products formed in the oxidation reactions of thioanisole by $[(N4Py)Fe^{IV}(O)]^{2+}$, which were carried out in the absence and presence of $HClO_4$ under Ar atmosphere in MeCN at 298 K, were analyzed by HPLC. Quantitative analyses were performed on the basis of comparison of HPLC peak integration between products and their authentic samples. In the case of thioanisole, methyl phenyl sulfoxide was obtained as a sole product with 96% and 93% yield (based on the

intermediate generated) in the absence and presence of $HClO_4$ (10 mM), respectively. In the cases of *para*-substituted thioanisoles, methyl *para*-substituted phenyl sulfoxides were obtained quantitatively by HPLC, as in the case of thioanisole.

Instrumentation. UV–vis spectra were recorded on a UNISOKU RSP-601 stopped-flow spectrometer equipped with a MOS-type highly sensitive photodiode array or a Hewlett-Packard 8453 photodiode-array spectrophotometer. X-band EPR spectra were taken at 5 K using a X-band Bruker EMX-plus spectrometer equipped with a dual mode cavity (ER 4116DM). Low temperatures were achieved and controlled with an Oxford Instruments ESR900 liquid He quartz cryostat with an Oxford Instruments ITC503 temperature and gas flow controller. The experimental parameters for EPR spectra were as follows: microwave frequency = 9.65 GHz, microwave power = 1 mW, modulation amplitude = 10 G, gain = 5×10^3 , time constant = 40.96 ms, conversion time = 81.00 ms. Electrospray ionization mass spectra (ESI MS) were collected on a Thermo Finnigan (San Jose, CA, USA) LCQ Advantage MAX quadrupole ion trap instrument, by infusing samples directly into the source using a manual method. The spray voltage was set at 3.7 kV and the capillary temperature at 100 °C. Product analysis for oxidation reactions was performed on a DIONEX Summit Pump Series P580 equipped with a variable wavelength UV-200 detector (HPLC). Products were separated on a Hypersil GOLD column (4.6 mm \times 250 mm), and product yields were determined with a UV Detector at 215 and 254 nm. 1H NMR spectra were measured with a Bruker model digital AVANCE III 400 FT-NMR spectrometer. Cyclic voltammetry (CV) measurements were performed on a BAS 630B electrochemical analyzer in a deaerated MeCN solution containing 0.10 M TBA(PF_6) as a supporting electrolyte at 298 K. A conventional three-electrode cell was used with a platinum working electrode, a platinum wire as a counter electrode, and a Ag/AgNO₃ reference electrode. The measured potentials were recorded with respect to the Ag/AgNO₃ (1.0×10^{-2} M). The E_{ox} and E_{red} values (vs Ag/AgNO₃) are converted to those vs SCE by adding 0.29 V.⁴⁰ All electrochemical measurements were carried out under an Ar atmosphere.

RESULTS AND DISCUSSION

Brønsted Acid-Promoted Oxygen Atom Transfer from $[(N4Py)Fe^{IV}(O)]^{2+}$ to Thioanisoles. It has been well established that oxygen atom transfer from a non-heme iron(IV)-oxo complex ($[(N4Py)Fe^{IV}(O)]^{2+}$) to thioanisole occurs to yield the sulfoxide and $[(N4Py)Fe^{II}]^{2+}$ in MeCN (see Figure S1 in the Supporting Information (SI) for ESI-MS).³⁹ The UV–visible spectral change observed in the reaction of oxygen atom transfer from $[(N4Py)Fe^{IV}(O)]^{2+}$ to thioanisole is shown in Figure 1a (left panel), where the absorption band at 695 nm due to $[(N4Py)Fe^{IV}(O)]^{2+}$ decreases, accompanied by increase in absorbance due to $[(N4Py)Fe^{II}]^{2+}$.



Addition of $HClO_4$ (70%, 10 mM) to an MeCN solution of $[(N4Py)Fe^{IV}(O)]^{2+}$ resulted in remarkable enhancement of the reaction rate, as indicated by the comparison of the time profile in the absence of $HClO_4$ (right panel in Figure 1a) vs that in the presence of $HClO_4$ (right panel in Figure 1b). In the presence of $HClO_4$, the reaction rate was too fast to follow by a conventional spectroscopic method; therefore, the rate was followed by using a stopped-flow technique (see Experimental Section). The rapid decrease in absorbance at 695 nm due to $[(N4Py)Fe^{IV}(O)]^{2+}$ in the presence of $HClO_4$ was accompanied by an increase in absorbance due to $[(N4Py)Fe^{II}]^{2+}$, which was observed as the recovery of the bleaching as shown in Figure 1b (right panel), where the spectrum after the

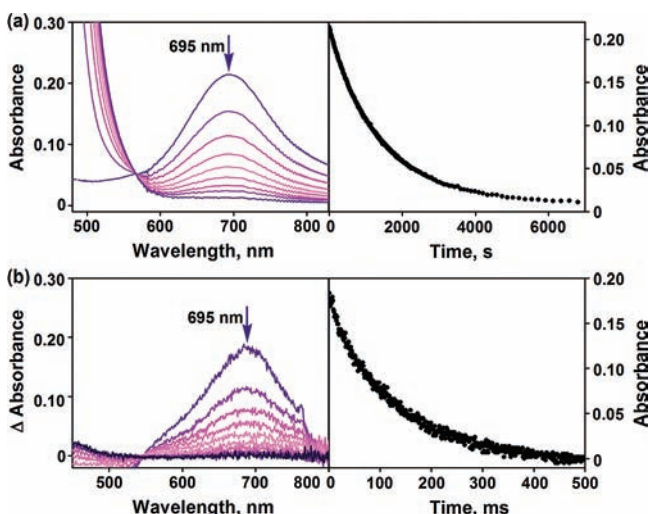


Figure 1. Visible spectral changes observed in the reaction of $[(N4Py)Fe^{IV}(O)]^{2+}$ (0.50 mM) with 10 equiv of thioanisole (5.0 mM) in the absence (a) and presence (b) of $HClO_4$ (10.0 mM) in MeCN at 298 K (left panel). Right panels show time courses monitored at 695 nm due to the decay of $[(N4Py)Fe^{IV}(O)]^{2+}$.

reaction was subtracted from the observed spectra in the stopped flow measurements. The yield of the sulfoxide in the presence of $HClO_4$ was quantitative, as is the case in the absence of $HClO_4$ (see Experimental Section).

Decay rates of the absorption band at 695 nm due to $[(N4Py)Fe^{IV}(O)]^{2+}$ in oxygen atom transfer from $[(N4Py)Fe^{IV}(O)]^{2+}$ to large excess thioanisole in the absence and presence of large excess $HClO_4$ obeyed pseudo-first-order kinetics (Figure 1). The pseudo-first-order rate constant increased linearly with increasing concentration of thioanisole (Figure S2 in the Supporting Information).⁴¹ The observed second-order rate constant (k_{obs}) obtained from the slope of a linear plot of the pseudofirst-order rate constant vs concentration of thioanisole increased proportionally with increasing concentration

of $HClO_4$ as shown in Figure 2a. The dependence of k_{obs} of other thioanisole derivatives on concentration of $HClO_4$ also exhibited linear relations (Figures 2b–d) as given by eq 2,

$$k_{obs} = k_0 + k_1[HClO_4] \quad (2)$$

where k_0 and k_1 are the rate constant of oxygen atom transfer from $[(N4Py)Fe^{IV}(O)]^{2+}$ to *para*-X-substituted thioanisoles in the absence and presence of $HClO_4$, respectively. The observed second-order rate constants (k_{obs}) of sulfoxidation of thioanisoles by $[(N4Py)Fe^{IV}(O)]^{2+}$ in the absence and presence of $HClO_4$ (10 mM) are listed in Table 1.

Table 1. One-Electron Oxidation Potentials (E_{ox}) of *para*-X-Substituted Thioanisoles and Second-Order Rate Constants of the Sulfoxidation by $[(N4Py)Fe^{IV}(O)]^{2+}$ in the Absence and Presence of $HClO_4$ (10 mM) in MeCN at 298 K

X	E_{ox} (vs SCE, V)	k_{obs} , $M^{-1} s^{-1}$	
		without $HClO_4$	with $HClO_4$ (10 mM)
Me	1.24	1.3 ± 0.1	$(3.2 \pm 0.2) \times 10^3$
H	1.34	$(8.7 \pm 0.4) \times 10^{-1}$	$(1.5 \pm 0.1) \times 10^3$
Cl	1.37	$(8.7 \pm 0.4) \times 10^{-1}$	$(7.2 \pm 0.4) \times 10^2$
Br	1.41	$(1.5 \pm 0.1) \times 10^{-1}$	$(8.4 \pm 0.4) \times 10^2$
CN	1.61	$(4.4 \pm 0.2) \times 10^{-2}$	$(6.2 \pm 0.3) \times 10$

It should be noted that the k_{obs} values of thioanisoles in the presence of $HClO_4$ (10 mM) are more than 10^3 -fold larger than the corresponding values in the absence of $HClO_4$. The enhanced reactivity of $[(N4Py)Fe^{IV}(O)]^{2+}$ by the presence of $HClO_4$ (70%) remarkably decreased by addition of H_2O . The k_{obs} value of acid-promoted sulfoxidation of thioanisole by $[(N4Py)Fe^{IV}(O)]^{2+}$ decreased significantly with increasing concentration of added water due to the decrease in the acidity of $HClO_4$ by H_2O ,^{12a,42} as shown in Figure 3. Because 70 wt % $HClO_4$ in H_2O is employed in this work, the use of 100% $HClO_4$ may enhance the reactivity of $[(N4Py)Fe^{IV}(O)]^{2+}$ drastically. However, the possible explosion of 100% $HClO_4$

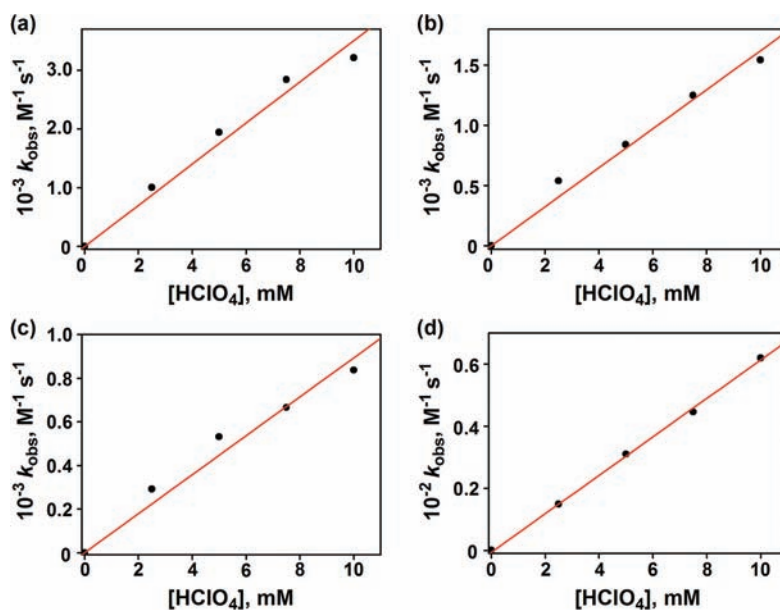


Figure 2. Plots of k_{obs} vs $HClO_4$ concentration in acid-promoted sulfoxidation of *para*-X-substituted thioanisoles (X = (a) Me, (b) H, (c) Br and (d) CN) by $[(N4Py)Fe^{IV}(O)]^{2+}$ in MeCN at 298 K.

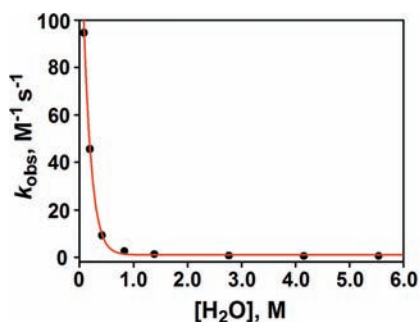


Figure 3. Plot of k_{obs} vs additional H_2O concentration in sulfoxidation of thioanisoles by $[(\text{N4Py})\text{Fe}^{\text{IV}}(\text{O})]^{2+}$ in the presence of HClO_4 (10 mM) in MeCN at 298 K.

has precluded the examination of the enhancement of reactivity of $[(\text{N4Py})\text{Fe}^{\text{IV}}(\text{O})]^{2+}$ by HClO_4 without water.

PCET from One-Electron Reductants to $[(\text{N4Py})\text{Fe}^{\text{IV}}(\text{O})]^{2+}$. When $[\text{Ru}^{\text{II}}(\text{Clphen})_3]^{2+}$ (Clphen: 5-chlorophenanthrene) was employed as an electron donor, no electron transfer from $[\text{Ru}^{\text{II}}(\text{Clphen})_3]^{2+}$ ($E_{\text{ox}} = 1.36$ V vs SCE)³⁰ to $[(\text{N4Py})\text{Fe}^{\text{IV}}(\text{O})]^{2+}$ ($E_{\text{red}} = 0.51$ V)³⁶ occurred in MeCN, because the free energy change of electron transfer is highly positive ($\Delta G_{\text{et}} = 0.85$ eV), i.e., endergonic. In the presence of HClO_4 , however, the electron transfer occurred efficiently as shown in Figure 4, where the absorption band due to $[\text{Ru}^{\text{II}}(\text{Clphen})_3]^{2+}$

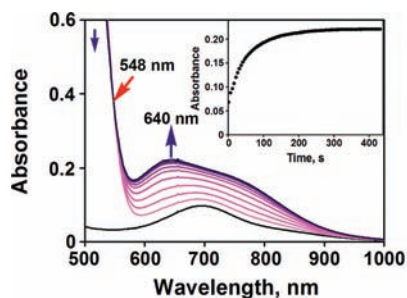


Figure 4. Visible spectral changes observed in PCET from $[\text{Ru}^{\text{II}}(\text{Clphen})_3]^{2+}$ (12.5 mM) to $[(\text{N4Py})\text{Fe}^{\text{IV}}(\text{O})]^{2+}$ (0.25 mM) in the presence of HClO_4 (10 mM) in MeCN at 298 K. The inset shows the time course monitored at 640 nm due to the formation of $[\text{Ru}^{\text{III}}(\text{Clphen})_3]^{3+}$.

($\lambda_{\text{max}} = 450$ nm) and $[(\text{N4Py})\text{Fe}^{\text{IV}}(\text{O})]^{2+}$ ($\lambda_{\text{max}} = 695$ nm) decreases to be changed to an absorption band due to $[\text{Ru}^{\text{III}}(\text{Clphen})_3]^{3+}$ ($\lambda_{\text{max}} = 640$ nm) with an isosbestic point at 548 nm.

Formation of $[\text{Ru}^{\text{III}}(\text{Clphen})_3]^{3+}$ and $[(\text{N4Py})\text{Fe}^{\text{III}}(\text{OH}_2)]^{3+}$ in the PCET reaction was confirmed by EPR measurements. In the absence of HClO_4 , as shown in Figure 5a, no electron transfer occurred because both reactants $[\text{Ru}^{\text{II}}(\text{Clphen})_3]^{2+}$ and $[(\text{N4Py})\text{Fe}^{\text{IV}}(\text{O})]^{2+}$ are EPR silent. In the presence of HClO_4 , PCET from $[\text{Ru}^{\text{II}}(\text{Clphen})_3]^{2+}$ to $[(\text{N4Py})\text{Fe}^{\text{IV}}(\text{O})]^{2+}$ occurred to produce $[\text{Ru}^{\text{III}}(\text{Clphen})_3]^{3+}$ and $[(\text{N4Py})\text{Fe}^{\text{III}}(\text{OH}_2)]^{3+}$, as indicated by EPR signals observed at $g_1 = 2.70$, $g_2 = 2.46$, and $g_3 = 1.65$ after the PCET reaction (Figure 5b). The observed EPR signals agree with the superposition of the EPR signals of $[\text{Ru}^{\text{III}}(\text{Clphen})_3]^{3+}$ (Figure 5c)⁴³ and $[(\text{N4Py})\text{Fe}^{\text{III}}(\text{OH}_2)]^{3+}$ (Figure 5d), which were produced by the photosensitized oxidation of $[\text{Ru}^{\text{II}}(\text{Clphen})_3]^{2+}$ with sodium persulfate and by

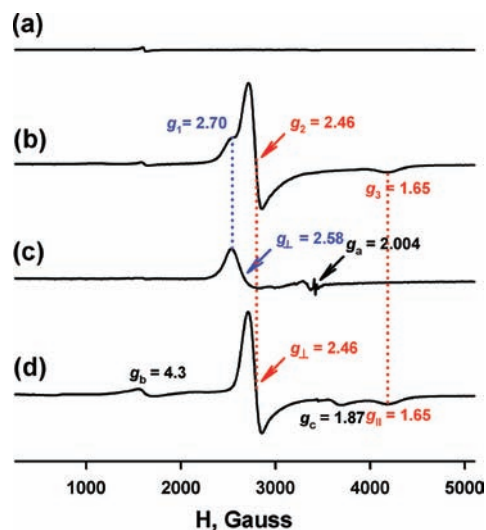


Figure 5. EPR spectra of the products obtained in the reaction of $[(\text{N4Py})\text{Fe}^{\text{IV}}(\text{O})]^{2+}$ (1.0 mM) with $[\text{Ru}^{\text{II}}(\text{Clphen})_3]^{2+}$ (2.0 mM) (a) in the absence and (b) presence of HClO_4 (10 mM). (c) EPR spectrum of $[\text{Ru}^{\text{III}}(\text{Clphen})_3]^{3+}$ generated in the photocatalytic oxidation of $[\text{Ru}^{\text{II}}(\text{Clphen})_3]^{2+}$ (1.0 mM) with sodium persulfate (50 mM) in the presence of HClO_4 (50 mM) in MeCN at 298 K. The EPR signal intensity observed at $g = 2.004$, which is attributed an organic radical species, is negligible as compared with the intensity due to $[\text{Ru}^{\text{III}}(\text{Clphen})_3]^{3+}$. (d) EPR spectrum of $[(\text{N4Py})\text{Fe}^{\text{III}}(\text{OH}_2)]^{3+}$ generated by PCET from ferrocene (1.0 mM) to $[(\text{N4Py})\text{Fe}^{\text{IV}}(\text{O})]^{2+}$ (1.0 mM) in the presence of HClO_4 (10 mM) in MeCN at 298 K. The low spin $[(\text{N4Py})\text{Fe}^{\text{III}}(\text{OH}_2)]^{3+}$ observed at $g_1 = 2.46$ and $g_2 = 1.65$ was converted to a high spin species at $g_b = 4.3$ and $g_c = 1.87$ at prolonged reaction time.

PCET from ferrocene to $[(\text{N4Py})\text{Fe}^{\text{IV}}(\text{O})]^{2+}$ in the presence of HClO_4 in MeCN at 298 K, respectively. It was observed that the low spin EPR signals due to $[(\text{N4Py})\text{Fe}^{\text{III}}(\text{OH}_2)]^{3+}$ were converted to the high spin EPR signals (g_b and g_c), which can be assigned to $[(\text{N4Py})\text{Fe}^{\text{III}}]^{3+}$.

The concentration of $[\text{Ru}^{\text{III}}(\text{Clphen})_3]^{3+}$ produced in PCET from $[\text{Ru}^{\text{II}}(\text{Clphen})_3]^{2+}$ to $[(\text{N4Py})\text{Fe}^{\text{IV}}(\text{O})]^{2+}$ (2.5×10^{-4} M) in the presence of HClO_4 (10 mM) increased with increasing the initial concentration of $[\text{Ru}^{\text{II}}(\text{Clphen})_3]^{2+}$ to reach the initial concentration of $[(\text{N4Py})\text{Fe}^{\text{IV}}(\text{O})]^{2+}$ as shown in Figure 6.

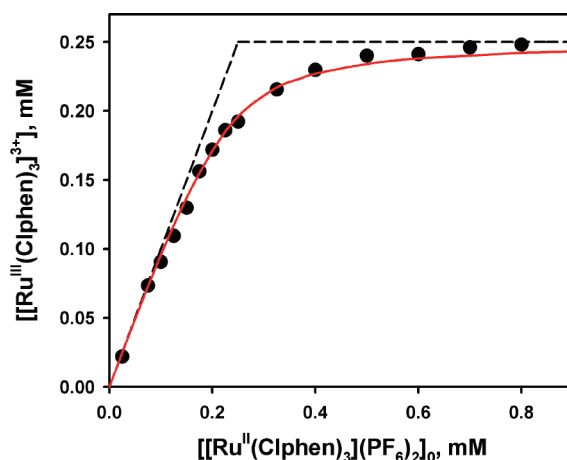
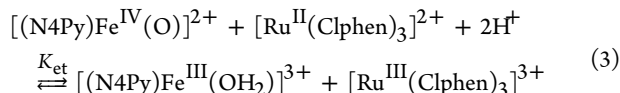


Figure 6. Plot of concentration of $[\text{Ru}^{\text{III}}(\text{Clphen})_3]^{3+}$ produced in PCET from $[\text{Ru}^{\text{II}}(\text{Clphen})_3]^{2+}$ to $[(\text{N4Py})\text{Fe}^{\text{IV}}(\text{O})]^{2+}$ (2.5×10^{-4} M) in the presence of HClO_4 (1.0×10^{-2} M) in deaerated MeCN at 298 K vs initial concentration of $[\text{Ru}^{\text{II}}(\text{Clphen})_3]^{2+}$, $[\text{Ru}^{\text{II}}(\text{Clphen})_3](\text{PF}_6)_2$.

Such a titration curve indicates that PCET from $[\text{Ru}^{\text{II}}(\text{Clphen})_3]^{2+}$ ($E_{\text{ox}} = 1.36 \text{ V vs SCE}$)³⁰ to $[(\text{N4Py})\text{Fe}^{\text{IV}}(\text{O})]^{2+}$ in the presence of HClO_4 (10 mM) is in equilibrium as shown in eq 3. The PCET equilibrium constant (K_{et}) was determined to be 14.0 by a fitting curve based on the PCET equilibrium (eq 3); see the Supporting Information for determination of K_{et} .



The reduction potential (E_{red}) of $[(\text{N4Py})\text{Fe}^{\text{IV}}(\text{O})]^{2+}$ in the presence of HClO_4 (10 mM) in MeCN at 298 K was then determined from the K_{et} value and E_{ox} value of $[\text{Ru}^{\text{II}}(\text{Clphen})_3]^{2+}$ ($E_{\text{ox}} = 1.36 \text{ V vs SCE}$)³⁰ using the Nernst equation (eq 4, where R

$$E_{\text{red}} = E_{\text{ox}} + (RT/F) \ln K_{\text{et}} \quad (4)$$

is the gas constant, T is absolute temperature, and F is the Faraday constant) to be 1.43 V vs SCE. The K_{et} values in the presence of various concentrations of HClO_4 were determined by global fitting of plots of concentrations of $[\text{Ru}^{\text{III}}(\text{Clphen})_3]^{3+}$ vs initial concentrations of $[\text{Ru}^{\text{II}}(\text{Clphen})_3]^{2+}$ (Figure S4 in the Supporting Information). The one-electron reduction potentials of $[(\text{N4Py})\text{Fe}^{\text{IV}}(\text{O})]^{2+}$ (E_{red}) in the presence of various concentrations of HClO_4 were also determined from the K_{et} values and the E_{ox} value of $[\text{Ru}^{\text{II}}(\text{Clphen})_3]^{2+}$ using eq 4.

The dependence of E_{red} of $[(\text{N4Py})\text{Fe}^{\text{IV}}(\text{O})]^{2+}$ on $\log([\text{HClO}_4])$ is shown in Figure 7, where the slope of the apparent linear

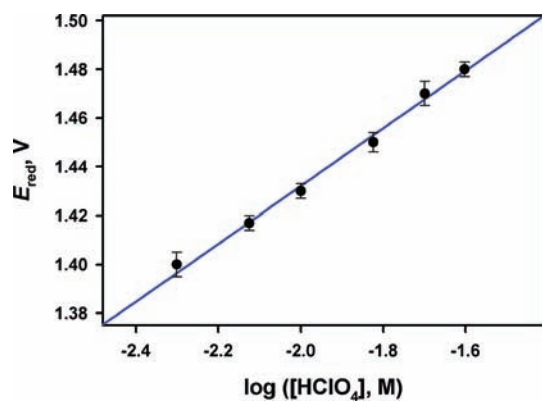


Figure 7. Dependence of E_{red} of $[(\text{N4Py})\text{Fe}^{\text{IV}}(\text{O})]^{2+}$ on $\log([\text{HClO}_4])$ in deaerated MeCN at 298 K. The blue line is fitted by eq 6.

correlation is close to $120 \text{ mV}/\log([\text{HClO}_4])$. This slope indicates that two protons are involved in the PCET reduction of $[(\text{N4Py})\text{Fe}^{\text{IV}}(\text{O})]^{2+}$ according to the Nernst equation for the dependence of E_{red} on $[\text{HClO}_4]$ (eq 5), where K_{red1} and K_{red2}

$$E_{\text{red}} = E_{\text{red}}^{\circ} + (2.3RT/F) \log(K_{\text{red1}}[\text{HClO}_4] \times (1 + K_{\text{red2}}[\text{HClO}_4])) \quad (5)$$

are the equilibrium constants for the first protonation and the second protonation of the one-electron reduced complex, $[(\text{N4Py})\text{Fe}^{\text{III}}(\text{O})]^{+}$.⁴⁴ The plot of E_{red} of $[(\text{N4Py})\text{Fe}^{\text{IV}}(\text{O})]^{2+}$ vs $\log([\text{HClO}_4])$ in Figure 7 is well fitted by eq 5 with the best fit values of K_{red1} and K_{red2} (1.2×10^{13} and $3.0 \times 10^6 \text{ M}^{-1}$,

respectively) as shown in the solid line (Figure 7). Under the conditions such that $K_{\text{red2}}[\text{HClO}_4] \gg 1$, eq 5 is rewritten by eq 6, when the slope of a linear correlation between E_{red} and $\log([\text{HClO}_4])$ corresponds to $2(2.3RT/F) = 118 \text{ mV}$ at 298 K, as observed in Figure 7.

$$E_{\text{red}} = E_{\text{red}}^{\circ} + 2(2.3RT/F) \log(K_{\text{red1}}K_{\text{red2}}[\text{HClO}_4]) \quad (6)$$

The protonation of two protons to $[(\text{N4Py})\text{Fe}^{\text{III}}(\text{O})]^{+}$ is also supported by the kinetic measurements (vide infra).²¹ The rate of PCET from $[\text{Fe}^{\text{II}}(\text{Me}_2\text{bpy})_3]^{2+}$ to $[(\text{N4Py})\text{Fe}^{\text{IV}}(\text{O})]^{2+}$ was determined by monitoring a decrease in absorbance at 695 nm due to $[(\text{N4Py})\text{Fe}^{\text{IV}}(\text{O})]^{2+}$. The rate obeyed pseudo-first-order kinetics in the presence of large excess $[\text{Fe}^{\text{II}}(\text{Me}_2\text{bpy})_3]^{2+}$ and HClO_4 (Figure S5 in the Supporting Information). The pseudo-first-order rate constant increased linearly with increasing concentration of $[\text{Fe}^{\text{II}}(\text{Me}_2\text{bpy})_3]^{2+}$ (Figure S6 in the Supporting Information). From the slope, the second-order rate constant (k_{et}) of PCET was determined. The k_{et} values of PCET from various one-electron reductants to $[(\text{N4Py})\text{Fe}^{\text{IV}}(\text{O})]^{2+}$ were determined from the slopes of k_1 vs concentrations of reductants. The k_{et} values increased with increasing concentration of HClO_4 and showed second-order dependence at the high concentration of HClO_4 , as shown in Figure 8.

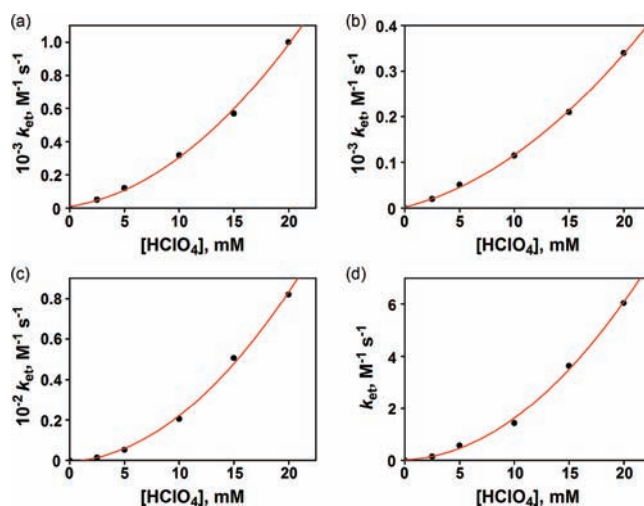


Figure 8. Plots of k_{et} vs concentrations of HClO_4 in PCET from (a) $[\text{Fe}^{\text{II}}(\text{Me}_2\text{bpy})_3](\text{PF}_6)_2$, (b) $[\text{Ru}^{\text{II}}(\text{Me}_2\text{bpy})_3](\text{PF}_6)_2$, (c) $[\text{Fe}^{\text{II}}(\text{Clphen})_3](\text{PF}_6)_2$, and (d) $[\text{Ru}^{\text{II}}(\text{Clphen})_3](\text{PF}_6)_2$ to $[(\text{N4Py})\text{Fe}^{\text{IV}}(\text{O})]^{2+}$ in the presence of HClO_4 (70%) in MeCN at 298 K.

This result shows sharp contrast to the case of proton-promoted oxygen atom transfer from $[(\text{N4Py})\text{Fe}^{\text{IV}}(\text{O})]^{2+}$ to thioanisoles in Figure 2, where the k_{obs} values increased linearly with increasing concentration of HClO_4 .

The results in Figure 8 are well analyzed by eq 7, where k_{et1} is the rate constant of electron transfer from a one-electron

$$k_{\text{et}} = k_{\text{et1}}[\text{HClO}_4] + k_{\text{et2}}[\text{HClO}_4]^2 \quad (7)$$

reductant to the monoprotonated complex ($[(\text{N4Py})\text{Fe}^{\text{IV}}(\text{OH})]^{3+}$) and k_{et2} is the rate constant of electron transfer to the diprotonated complex ($[(\text{N4Py})\text{Fe}^{\text{IV}}(\text{OH}_2)]^{4+}$). Equation 7 is written by eq 8, which predicts a linear relation

between $k_{\text{et}}/([\text{HClO}_4])$ and $[\text{HClO}_4]$. Linear plots of $k_{\text{et}}/([\text{HClO}_4])$ and $[\text{HClO}_4]$ were confirmed as shown in Figure 9,

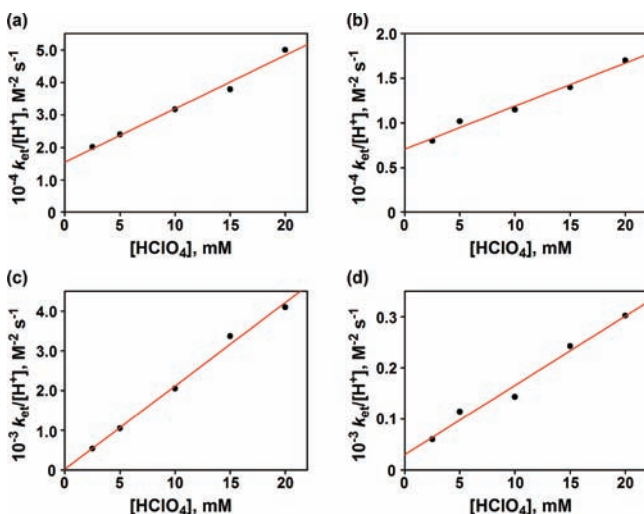


Figure 9. Plots of $k_{\text{et}}/[\text{HClO}_4]$ vs $[\text{HClO}_4]$ in PCET from (a) $[\text{Fe}^{\text{II}}(\text{Me}_2\text{bpy})_3](\text{PF}_6)_2$, (b) $[\text{Ru}^{\text{II}}(\text{Me}_2\text{bpy})_3](\text{PF}_6)_2$, (c) $[\text{Fe}^{\text{II}}(\text{Clphen})_3](\text{PF}_6)_2$, and (d) $[\text{Ru}^{\text{II}}(\text{Clphen})_3](\text{PF}_6)_2$ to $[(\text{N4Py})\text{Fe}^{\text{IV}}(\text{O})]^{2+}$ in the presence of HClO_4 in MeCN at 298 K.

indicating the involvement of two protons in the PCET reactions.

$$k_{\text{et}}/[\text{HClO}_4] = k_{\text{et}1} + k_{\text{et}2}[\text{HClO}_4] \quad (8)$$

Direct Oxygen Atom Transfer vs Electron Transfer in Proton-Promoted Sulfoxidation of Thioanisoles by $[(\text{N4Py})\text{Fe}^{\text{IV}}(\text{O})]^{2+}$. The first-order dependence of k_{obs} of the acid-promoted oxygen atom transfer from $[(\text{N4Py})\text{Fe}^{\text{IV}}(\text{O})]^{2+}$ to thioanisoles on $[\text{HClO}_4]$ in Figure 2 suggests that the rate-determining step of the acid promoted oxygen atom transfer cannot be PCET from thioanisoles to $[(\text{N4Py})\text{Fe}^{\text{IV}}(\text{O})]^{2+}$, because the PCET rate constants exhibit a second-order dependence on $[\text{HClO}_4]$ (Figure 8). The mechanistic difference between proton-promoted oxygen atom transfer and PCET can be clarified by comparing the dependence of k_{obs} vs k_{et} on the PCET driving force (vide infra).

The PCET driving force ($-\Delta G_{\text{et}}$) was obtained from the difference between the one-electron oxidation potentials of thioanisoles (E_{ox} vs SCE)⁴⁵ and the one-electron reduction potentials of $[(\text{N4Py})\text{Fe}^{\text{IV}}(\text{O})]^{2+}$ (E_{red} vs SCE) in the absence and presence of HClO_4 at 298 K.³⁶ It should be noted that the E_{ox} values of thioanisoles are not changed in the presence of HClO_4 , whereas the E_{red} value of $[(\text{N4Py})\text{Fe}^{\text{IV}}(\text{O})]^{2+}$ is significantly shifted to the positive direction from 0.51 V vs SCE in the absence of HClO_4 to 1.43 V vs SCE in the presence of 10 mM of HClO_4 (vide supra).³⁶

The driving force dependence of rate constants of PCET from one-electron reductants to $[(\text{N4Py})\text{Fe}^{\text{IV}}(\text{O})]^{2+}$ in the presence of 10 mM HClO_4 is well fitted in light of the Marcus theory of adiabatic outer-sphere electron transfer (eq 9), where

$$k_{\text{et}} = Z \exp[-(\lambda/4)(1 + \Delta G_{\text{et}}/\lambda)^2/k_{\text{B}}T] \quad (9)$$

Z is the collision frequency, taken as $1 \times 10^{11} \text{ M}^{-1} \text{ s}^{-1}$, λ is the reorganization energy of electron transfer, k_{B} is the Boltzmann constant, and T is the absolute temperature.³⁵ The best fit λ value of PCET from one-electron reductants to $[(\text{N4Py})\text{Fe}^{\text{IV}}(\text{O})]^{2+}$ in

the presence of 10 mM HClO_4 is determined to be 2.74 eV, which is the same as the λ value of electron transfer from one-electron reductants to $[(\text{N4Py})\text{Fe}^{\text{IV}}(\text{O})]^{2+}$ (2.74 eV) as shown in Figure 10.³⁶ The same value of the reorganization energy

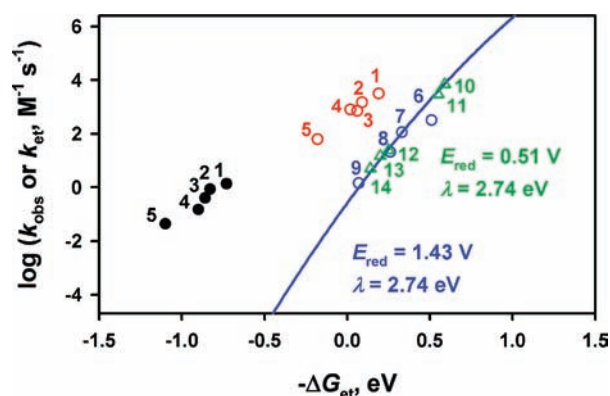


Figure 10. Plots of $\log k_{\text{obs}}$ for sulfoxidation of *para*-X-substituted thioanisoles (X = (1) Me, (2) H, (3) Cl, (4) Br, and (5) CN) by $[(\text{N4Py})\text{Fe}^{\text{IV}}(\text{O})]^{2+}$ in the absence and presence of HClO_4 (70%, 10 mM) MeCN at 298 K vs the driving force of electron transfer $[-\Delta G = e(E_{\text{red}} - E_{\text{ox}})]$ from thioanisoles to $[(\text{N4Py})\text{Fe}^{\text{IV}}(\text{O})]^{2+}$ in the absence (black closed circles) and the presence of HClO_4 (10 mM) (red open circles). The blue open circles show the driving force dependence of the rate constants ($\log k_{\text{et}}$) of PCET from one-electron reductants ((6) $[\text{Fe}^{\text{II}}(\text{Me}_2\text{bpy})_3](\text{PF}_6)_2$, (7) $[\text{Ru}^{\text{II}}(\text{Me}_2\text{bpy})_3](\text{PF}_6)_2$, (8) $[\text{Fe}^{\text{II}}(\text{Clphen})_3](\text{PF}_6)_2$, and (9) $[\text{Ru}^{\text{II}}(\text{Clphen})_3](\text{PF}_6)_2$) to $[(\text{N4Py})\text{Fe}^{\text{IV}}(\text{O})]^{2+}$ in the presence of HClO_4 (10 mM) in MeCN at 298 K (see Table S1 in the Supporting Information). The green open triangles show the driving force dependence of the rate constants ($\log k_{\text{et}}$) of electron transfer from one-electron reductants ((10) decamethylferrocene, (11) octamethylferrocene, (12) 1,1'-dimethylferrocene, (13) *n*-amylferrocene, and (14) ferrocene) to $[(\text{N4Py})\text{Fe}^{\text{IV}}(\text{O})]^{2+}$ in the absence of HClO_4 in MeCN at 298 K.³⁴

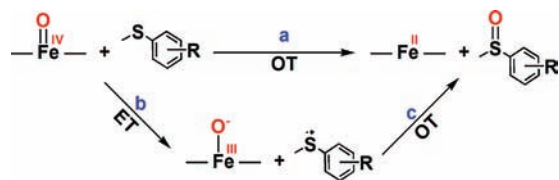
(2.74 eV) obtained from electron transfer from one-electron reductants to $[(\text{N4Py})\text{Fe}^{\text{IV}}(\text{O})]^{2+}$ ($[(\text{N4Py})\text{Fe}^{\text{IV}}(\text{OH}_2)]^{4+}$) in the presence and absence of HClO_4 indicates that the large reorganization energy results from the one-electron reduction of the Fe^{IV} center to the Fe^{III} center. In fact, a large reorganization energy (2.34 eV) was reported for the electron-transfer oxidation of an organoiron(III) porphyrin to the corresponding organoiron(IV) porphyrin.⁴⁶

It is interesting to note that two Sc^{3+} ions are involved in Sc^{3+} -promoted electron transfer from one-electron reductants to $[(\text{N4Py})\text{Fe}^{\text{IV}}(\text{O})]^{2+}$ as the case of the PCET reactions of $[(\text{N4Py})\text{Fe}^{\text{IV}}(\text{O})]^{2+}$, in which two protons are also involved. The observed second-order rate constants of Sc^{3+} -promoted oxygen atom transfer from $[(\text{N4Py})\text{Fe}^{\text{IV}}(\text{O})]^{2+}$ to thioanisoles fit well with the driving force dependence of k_{et} for Sc^{3+} -promoted electron-transfer reactions using the Marcus equation (eq 9). Such an agreement with the Marcus equation indicates that the Sc^{3+} -promoted oxygen atom transfer from $[(\text{N4Py})\text{Fe}^{\text{IV}}(\text{O})]^{2+}$ to thioanisoles in the presence of Sc^{3+} proceeds via Sc^{3+} ion-coupled electron transfer from thioanisoles to $[(\text{N4Py})\text{Fe}^{\text{IV}}(\text{O})]^{2+}$, which is the rate-determining step, followed by rapid transfer of the oxygen atom from $[(\text{N4Py})\text{Fe}^{\text{III}}(\text{O})]^{+}$ to the radical cation ($\text{ArSR}^{\bullet+}$).³¹

In the absence of HClO_4 , the driving force of electron transfer ($-\Delta G_{\text{et}}$) is largely negative. This indicates that electron transfer from thioanisoles to $[(\text{N4Py})\text{Fe}^{\text{IV}}(\text{O})]^{2+}$ is highly endergonic and thereby the electron transfer is thermodynamically infeasible.

The k_{obs} values in the absence of HClO_4 are more than 10 orders magnitude larger than the expected k_{et} values of outer-sphere electron transfer from thioanisoles to $[(\text{N4Py})\text{Fe}^{\text{IV}}(\text{O})]^{2+}$ without HClO_4 (extrapolated blue line in Figure 10). In such a case, direct oxygen atom transfer (Scheme 1a) occurs

Scheme 1



rather than an outer-sphere electron-transfer pathway (Scheme 1b).³¹

In the presence of HClO_4 (10 mM), the k_{obs} values are still two to four orders magnitude larger than the expected k_{et} values of outer-sphere PCET from thioanisoles to $[(\text{N4Py})\text{Fe}^{\text{IV}}(\text{O})]^{2+}$ in the presence of HClO_4 (10 mM) (blue line in Figure 10). Thus, the proton-promoted sulfoxidation of thioanisoles also occurs via direct oxygen atom transfer from the monoprotonated complex $[(\text{N4Py})\text{Fe}^{\text{IV}}(\text{OH})]^{3+}$ to thioanisoles rather than outer-sphere PCET from thioanisoles to $[(\text{N4Py})\text{Fe}^{\text{IV}}(\text{O})]^{2+}$. The difference in the reaction pathways between proton-promoted direct oxygen atom transfer and Sc^{3+} ion-coupled electron transfer may result from the steric effect. Direct oxygen atom transfer from the monoprotonated complex $[(\text{N4Py})\text{Fe}^{\text{IV}}(\text{OH})]^{3+}$ to thioanisoles may be made possible by the small size of the proton, whereas the direct oxygen atom transfer from Sc^{3+} -bound complex $[(\text{N4Py})\text{Fe}^{\text{IV}}(\text{O})-\text{Sc}(\text{OTf})_3]^{2+}$ to thioanisoles may be prohibited due to the steric effect of bulky $\text{Sc}(\text{OTf})_3$ bound to the $\text{Fe}^{\text{IV}}(\text{O})$ complex. In the case of the $\text{Sc}(\text{OTf})_3$ -promoted reaction, only outer-sphere electron transfer can occur because outer-sphere electron transfer requires little interaction between electron donor and acceptor molecules, thereby being insensitive to steric effects. In both the Sc^{3+} ion-coupled electron transfer and PCET from one-electron reductants to $[(\text{N4Py})\text{Fe}^{\text{IV}}(\text{O})]^{2+}$, two Sc^{3+} ions and two protons are involved in the electron-transfer reactions, exhibiting the second-order dependence of the rate constant on concentrations of $\text{Sc}(\text{OTf})_3$ and HClO_4 , respectively. In the case of proton-promoted direct oxygen transfer, only the monoprotonated complex $[(\text{N4Py})\text{Fe}^{\text{IV}}(\text{OH})]^{3+}$ is involved and the diprotonated complex $[(\text{N4Py})\text{Fe}^{\text{IV}}(\text{OH}_2)]^{4+}$ is less reactive due to the steric effect of two protons, whereas, in the PCET reaction, the diprotonated complex $[(\text{N4Py})\text{Fe}^{\text{IV}}(\text{OH}_2)]^{4+}$ is the most reactive species because of the much higher reduction potential as indicated by eq 5. The proton-promoted direct oxygen transfer from thioanisoles to $[(\text{N4Py})\text{Fe}^{\text{IV}}(\text{OH})]^{3+}$ may be regarded as inner-sphere electron transfer,^{47–49} in which electron transfer is accompanied by the oxygen–ligand transfer.⁵⁰

CONCLUSION

We have found that sulfoxidation of thioanisoles by a non-heme iron(IV)–oxo complex $[(\text{N4Py})\text{Fe}^{\text{IV}}(\text{O})]^{2+}$ is remarkably promoted by a Brønsted acid (HClO_4). The comparison of the observed second-order rate constants of acid-promoted sulfoxidation of thioanisoles by $[(\text{N4Py})\text{Fe}^{\text{IV}}(\text{O})]^{2+}$ with those of PCET from one-electron reductants to $[(\text{N4Py})\text{Fe}^{\text{IV}}(\text{O})]^{2+}$ in light of the Marcus theory of outer-sphere electron transfer has allowed

us to conclude that acid-promoted sulfoxidation of thioanisoles by $[(\text{N4Py})\text{Fe}^{\text{IV}}(\text{O})]^{2+}$ proceeds via direct oxygen atom transfer from the monoprotonated complex $[(\text{N4Py})\text{Fe}^{\text{IV}}(\text{OH})]^{3+}$ to thioanisoles rather than outer-sphere PCET from thioanisoles to $[(\text{N4Py})\text{Fe}^{\text{IV}}(\text{O})]^{2+}$. Such an activation of $\text{Fe}^{\text{IV}}=\text{O}$ species by the protonation will expand the scope of acid-promoted reactions of high-valent metal–oxo complexes as the case of organic compounds containing a $\text{C}=\text{O}$ bond.

ASSOCIATED CONTENT

Supporting Information

Table of oxidation potentials, reductants, and second-order rate constants; ESI-MS spectrum; ^1H NMR spectrum; concentration vs concentration plots; visible spectral changes during reactions; and plots of the pseudo-first-order rate constants vs concentrations. This material is available free of charge via the Internet at <http://pubs.acs.org>.

AUTHOR INFORMATION

Corresponding Author

fukuzumi@chem.eng.osaka-u.ac.jp; wwnam@ewha.ac.kr

Notes

The authors declare no competing financial interest.

ACKNOWLEDGMENTS

The research at OU was supported by Grant-in-Aid No. 19205019 to S.F. and Global COE program “the Global Education and Research Center for Bio-Environmental Chemistry” from the Ministry of Education, Culture, Sports, Science and Technology, Japan (to S.F.), and the research at EWU was supported by NRF/MEST of Korea through CRI (to W.N.), GRL (2010-00353) (to W.N.), 2011 KRICT OASIS project (to W.N.), and WCU (R31-2008-000-10010-0) (to W.N. and S.F.).

REFERENCES

- (1) (a) Akiyama, T. *Chem. Rev.* **2007**, *107*, 5744. (b) Akiyama, T.; Itoh, J.; Fuchibe, K. *Adv. Synth. Catal.* **2006**, *348*, 999. (c) Cheon, C.-H.; Yamamoto, H. *Chem. Commun.* **2011**, *47*, 3043.
- (2) (a) Yu, J.; Shi, F.; Gong, L.-Z. *Acc. Chem. Res.* **2011**, *44*, 1156. (b) Sun, J.; Kozmin, S. A. *J. Am. Chem. Soc.* **2005**, *127*, 13512. (c) Zhang, L.; Kozmin, S. A. *J. Am. Chem. Soc.* **2004**, *126*, 10204.
- (3) (a) Schreiner, P. R. *Chem. Soc. Rev.* **2003**, *32*, 289. (b) Pihko, P. M. *Angew. Chem., Int. Ed.* **2004**, *43*, 2062. (c) Bolm, C.; Rantanen, T.; Schiffrers, I.; Zani, L. *Angew. Chem., Int. Ed.* **2005**, *44*, 1758. (d) Pihko, P. M. *Lett. Org. Chem.* **2005**, *2*, 398. (e) Taylor, M. S.; Jacobsen, E. N. *Angew. Chem., Int. Ed.* **2006**, *45*, 1520. (f) Mahoney, J. M.; Smith, C. R.; Johnston, J. N. *J. Am. Chem. Soc.* **2005**, *127*, 1354.
- (4) (a) *Selectivities in Lewis Acid Promoted Reactions*; Schinzer, D., Ed.; Kluwer Academic: Dordrecht, 1989. (b) *Lewis Acids in Organic Synthesis*; Yamamoto, H., Ed.; Wiley-VCH: Weinheim, 2000. (c) Abell, J. P.; Yamamoto, H. *Chem. Soc. Rev.* **2010**, *39*, 61.
- (5) (a) Kobayashi, S.; Ishitani, H. *Chem. Rev.* **1999**, *99*, 1069. (b) Akiyama, R.; Kobayashi, S. *Chem. Rev.* **2009**, *109*, 594. (c) Kobayashi, S.; Yamashita, Y. *Acc. Chem. Res.* **2011**, *44*, 58.
- (6) (a) Johnson, J. S.; Evans, D. A. *Acc. Chem. Res.* **2000**, *33*, 325. (b) Rovis, T.; Evans, D. A. *Prog. Inorg. Chem.* **2001**, *50*, 1.
- (7) (a) Pohlhaus, P. D.; Bowman, R. K.; Johnson, J. S. *J. Am. Chem. Soc.* **2004**, *126*, 2294. (b) Fukuzumi, S.; Fujita, M.; Otera, J.; Fujita, Y. *J. Am. Chem. Soc.* **1992**, *114*, 10271.
- (8) (a) Mukaiyama, T.; Ishida, A. *Chem. Lett.* **1975**, 319. (b) Ishida, A.; Mukaiyama, T. *Chem. Lett.* **1975**, 1167. (c) Ishida, A.; Mukaiyama, T. *Bull. Chem. Soc. Jpn.* **1977**, *50*, 1161. (d) Ishida, A.; Mukaiyama, T. *Chem. Lett.* **1977**, 467. (e) Ishida, A.; Mukaiyama, T. *Bull. Chem. Soc. Jpn.* **1978**, *51*, 2077. (f) Mukaiyama, T.; Ishida, A. *Chem. Lett.* **1975**, 1201.

- (9) (a) Casiraghi, G.; Battistini, L.; Curti, C.; Rassa, G.; Zanardi, F. *Chem. Rev.* **2011**, *111*, 3076. (b) Denmark, S. E.; Heemstra, J. R. Jr.; Beutner, G. L. *Angew. Chem., Int. Ed.* **2005**, *44*, 4682. (c) Casiraghi, G.; Zanardi, F.; Appendino, G.; Rassa, G. *Chem. Rev.* **2000**, *100*, 1929. (d) Kalesse, M. *Top. Curr. Chem.* **2005**, *244*, 43.
- (10) (a) Fukuzumi, S. *Bull. Chem. Soc. Jpn.* **1997**, *70*, 1. (b) Fukuzumi, S. *Org. Biomol. Chem.* **2003**, *1*, 609. (c) Fukuzumi, S. *Bull. Chem. Soc. Jpn.* **2006**, *79*, 177. (d) Fukuzumi, S. *Pure Appl. Chem.* **2007**, *79*, 981. (e) Fukuzumi, S. *Pure Appl. Chem.* **2003**, *75*, 577.
- (11) (a) Fukuzumi, S.; Ishikawa, K.; Hironaka, K.; Tanaka, T. *J. Chem. Soc., Perkin Trans. 2* **1987**, 751. (b) Fukuzumi, S.; Ishikawa, M.; Tanaka, T. *Chem. Commun.* **1985**, 1069. (c) Fukuzumi, S.; Ishikawa, M.; Tanaka, T. *J. Chem. Soc., Perkin Trans. 2* **1989**, 1811. (d) Ishikawa, M.; Fukuzumi, S. *Chem. Commun.* **1990**, 1353. (e) Ishikawa, M.; Fukuzumi, S. *J. Chem. Soc., Faraday Trans. 1* **1990**, *86*, 3531. (f) Fukuzumi, S.; Mochizuki, S.; Tanaka, T. *J. Am. Chem. Soc.* **1989**, *111*, 1497. (g) Yuasa, J.; Yamada, S.; Fukuzumi, S. *J. Am. Chem. Soc.* **2008**, *130*, 5808.
- (12) (a) Fukuzumi, S.; Kuroda, S. *Res. Chem. Int.* **1999**, *25*, 789. (b) Fukuzumi, S.; Tokuda, Y. *J. Phys. Chem.* **1993**, *97*, 3737. (c) Fukuzumi, S.; Chiba, M. *J. Chem. Soc., Perkin Trans. 2* **1991**, 1393. (d) Fukuzumi, S.; Mochizuki, S.; Tanaka, T. *J. Phys. Chem.* **1990**, *94*, 722.
- (13) (a) Hayashi, H.; Ogo, S.; Fukuzumi, S. *Chem. Commun.* **2004**, 2714. (b) Hayashi, H.; Ogo, S.; Abura, T.; Fukuzumi, S. *J. Am. Chem. Soc.* **2003**, *125*, 14266.
- (14) (a) Halime, Z.; Kotani, H.; Li, Y.; Fukuzumi, S.; Karlin, K. D. *Proc. Natl. Acad. Sci. U.S.A.* **2011**, *108*, 13990. (b) Fukuzumi, S.; Okamoto, K.; Gros, C. P.; Guillard, R. *J. Am. Chem. Soc.* **2004**, *126*, 10441. (c) Fukuzumi, S.; Mochizuki, S.; Tanaka, T. *Inorg. Chem.* **1989**, *28*, 2459.
- (15) (a) Fukuzumi, S. *Prog. Inorg. Chem.* **2009**, *56*, 49. (b) Fukuzumi, S. *Bull. Chem. Soc. Jpn.* **1997**, *70*, 1. (c) Fukuzumi, S.; Ohtsu, H.; Ohkubo, K.; Itoh, S.; Imahori, H. *Coord. Chem. Rev.* **2002**, *226*, 71. (d) Fukuzumi, S.; Ohkubo, K. *Coord. Chem. Rev.* **2010**, *254*, 372.
- (16) (a) Fukuzumi, S.; Itoh, S. In *Advances in Photochemistry*; Neckers, D. C., Volman, D. H., von Büna, G., Eds.; Wiley: New York, 1998; Vol. 25, pp 107–172. (b) Fukuzumi, S.; Itoh, S. *Antioxid. Redox Signaling* **2001**, *3*, 807.
- (17) (a) Fukuzumi, S.; Ohkubo, K. *Chem.–Eur. J.* **2000**, *6*, 4532. (b) Ohkubo, K.; Menon, S.; Orita, C. A.; Otera, J.; Fukuzumi, S. *J. Org. Chem.* **2003**, *68*, 4720.
- (18) (a) Fukuzumi, S.; Okamoto, T. *J. Am. Chem. Soc.* **1993**, *115*, 11600. (b) Fukuzumi, S.; Nishizawa, N.; Tanaka, T. *J. Chem. Soc., Perkin Trans. 2* **1985**, 371. (c) Fukuzumi, S.; Suenobu, T.; Patz, M.; Hirasaka, T.; Itoh, S.; Fujitsuka, M.; Ito, O. *J. Am. Chem. Soc.* **1998**, *120*, 8060.
- (19) (a) Fukuzumi, S.; Kuroda, S.; Tanaka, T. *J. Am. Chem. Soc.* **1985**, *107*, 3020. (b) Itoh, S.; Taniguchi, M.; Takada, N.; Nagatomo, S.; Kitagawa, T.; Fukuzumi, S. *J. Am. Chem. Soc.* **2000**, *122*, 12087. (c) Fukuzumi, S.; Yasui, K.; Suenobu, T.; Ohkubo, K.; Fujitsuka, M.; Ito, O. *J. Phys. Chem. A* **2001**, *105*, 10501.
- (20) (a) Fukuzumi, S.; Okamoto, T.; Otera, J. *J. Am. Chem. Soc.* **1994**, *116*, 5503. (b) Fukuzumi, S.; Fujii, Y.; Suenobu, T. *J. Am. Chem. Soc.* **2001**, *123*, 10191.
- (21) (a) Itoh, S.; Kumei, H.; Nagatomo, S.; Kitagawa, T.; Fukuzumi, S. *J. Am. Chem. Soc.* **2001**, *123*, 2165. (b) Fukuzumi, S.; Satoh, N.; Okamoto, T.; Yasui, K.; Suenobu, T.; Seko, Y.; Fujitsuka, M.; Ito, O. *J. Am. Chem. Soc.* **2001**, *123*, 7756. (c) Fukuzumi, S.; Ohkubo, K.; Okamoto, T. *J. Am. Chem. Soc.* **2002**, *124*, 14147.
- (22) (a) Fukuzumi, S.; Okamoto, K.; Imahori, H. *Angew. Chem., Int. Ed.* **2002**, *41*, 620. (b) Okamoto, K.; Imahori, H.; Fukuzumi, S. *J. Am. Chem. Soc.* **2003**, *125*, 7014. (c) Fukuzumi, S.; Okamoto, K.; Yoshida, Y.; Imahori, H.; Araki, Y.; Ito, O. *J. Am. Chem. Soc.* **2003**, *125*, 1007. (d) Savéant, J.-M. *J. Am. Chem. Soc.* **2008**, *130*, 4732.
- (23) (a) Chen, X.; Bu, Y. *J. Am. Chem. Soc.* **2007**, *129*, 9713. (b) Wu, H.; Zhang, D.; Su, L.; Ohkubo, K.; Zhang, C.; Yin, S.; Mao, L.; Shuai, Z.; Fukuzumi, S.; Zhu, D. *J. Am. Chem. Soc.* **2007**, *129*, 6839. (c) Zeng, Y.; Zhang, G.; Zhang, D.; Zhu, D. *J. Org. Chem.* **2009**, *74*, 4375.
- (d) Jia, L.; Zhang, G.; Zhang, D.; Xiang, J.; Xu, W.; Zhu, D. *Chem. Commun.* **2011**, 47, 322.
- (24) (a) Yuasa, J.; Suenobu, T.; Fukuzumi, S. *J. Am. Chem. Soc.* **2003**, *125*, 12090. (b) Yuasa, J.; Suenobu, T.; Fukuzumi, S. *ChemPhysChem* **2006**, *7*, 942. (c) Yuasa, J.; Yamada, S.; Fukuzumi, S. *Chem.–Eur. J.* **2008**, *14*, 1866.
- (25) (a) Dempsey, J. L.; Winkler, J. R.; Gray, H. B. *Chem. Rev.* **2010**, *110*, 7024. (b) Warren, J. J.; Tronic, T. A.; Mayer, J. M. *Chem. Rev.* **2010**, *110*, 6961. (c) Huynh, M. H. V.; Meyer, T. J. *Chem. Rev.* **2007**, *107*, 5004.
- (26) (a) Reece, S. Y.; Nocera, D. G. *Annu. Rev. Biol. Chem.* **2009**, *78*, 673. (b) Chang, C. J.; Chang, M. C. Y.; Damrauer, N. H.; Nocera, D. G. *Biochim. Biophys. Acta* **2004**, *1655*, 13. (c) Cukier, R. I.; Nocera, D. G. *Annu. Rev. Phys. Chem.* **1998**, *49*, 337.
- (27) (a) Mayer, J. M.; Rhile, I. J. *Biochim. Biophys. Acta* **2004**, *1655*, 51. (b) Mayer, J. M. *Annu. Rev. Phys. Chem.* **2004**, *55*, 363.
- (28) Fukuzumi, S. *Helv. Chim. Acta* **2006**, *89*, 2425.
- (29) (a) Fukuzumi, S.; Morimoto, Y.; Kotani, H.; Naumov, P.; Lee, Y.-M.; Nam, W. *Nature Chem.* **2010**, *2*, 756. (b) Karlin, K. D. *Nature Chem.* **2010**, *2*, 711.
- (30) Morimoto, Y.; Kotani, H.; Park, J.; Lee, Y.-M.; Nam, W.; Fukuzumi, S. *J. Am. Chem. Soc.* **2011**, *133*, 403.
- (31) Park, J.; Morimoto, Y.; Lee, Y.-M.; Nam, W.; Fukuzumi, S. *J. Am. Chem. Soc.* **2011**, *133*, 5236.
- (32) Park, J.; Morimoto, Y.; Lee, Y.-M.; You, Y.; Nam, W.; Fukuzumi, S. *Inorg. Chem.* **2011**, *50*, 11612.
- (33) (a) Fukuzumi, S.; Kotani, H.; Suenobu, T.; Hong, S.; Lee, Y.-M.; Nam, W. *Chem.–Eur. J.* **2010**, *16*, 354. (b) Fukuzumi, S.; Kotani, H.; Prokop, K. A.; Goldberg, D. P. *J. Am. Chem. Soc.* **2011**, *133*, 1859.
- (34) (a) Lubben, M.; Meetsma, A.; Wilkinson, E. C.; Feringa, B.; Que, L. Jr. *Angew. Chem., Int. Ed.* **1995**, *34*, 1512. (b) Kaizer, J.; Klinker, E. J.; Oh, N. Y.; Rohde, J.-U.; Song, W. J.; Stubna, A.; Kim, J.; Müinck, E.; Nam, W.; Que, L. Jr. *J. Am. Chem. Soc.* **2004**, *126*, 472. (c) Klinker, E. J.; Kaizer, J.; Brennessel, W. W.; Woodrum, N. L.; Cramer, C. J.; Que, L. Jr. *Angew. Chem., Int. Ed.* **2005**, *44*, 3690.
- (35) (a) Marcus, R. A. *Annu. Rev. Phys. Chem.* **1964**, *15*, 155. (b) Marcus, R. A. *Angew. Chem., Int. Ed. Engl.* **1993**, *32*, 1111.
- (36) Lee, Y.-M.; Kotani, H.; Suenobu, T.; Nam, W.; Fukuzumi, S. *J. Am. Chem. Soc.* **2008**, *130*, 434.
- (37) (a) Arias, J.; Newlands, C. R.; Abu-Omar, M. M. *Inorg. Chem.* **2001**, *40*, 2185. (b) Prokop, K. A.; New, H. M.; de Visser, S. P.; Goldberg, D. P. *J. Am. Chem. Soc.* **2011**, *133*, 15874. (c) Fertinger, C.; Hessenauer-Ilicheva, N.; Franke, A.; van Eldik, R. *Chem.–Eur. J.* **2009**, *15*, 13435. (d) Arunkumar, C.; Lee, Y.-M.; Lee, J. Y.; Fukuzumi, S.; Nam, W. *Chem.–Eur. J.* **2009**, *15*, 11482. (e) Kumar, A.; Goldberg, I.; Botoshansky, M.; Buchman, Y.; Gross, Z. *J. Am. Chem. Soc.* **2010**, *132*, 15233. (f) Benet-Buchholz, J.; Comba, P.; Llobet, A.; Roeser, S.; Vadivelu, P.; Wiesner, S. *Dalton Trans.* **2010**, 39, 3315.
- (38) Armarego, W. L. F.; Chai, C. L. L. *Purification of Laboratory Chemicals*, 5th ed.; Butterworth Heinemann: Amsterdam, 2003.
- (39) Park, M. J.; Lee, J.; Suh, Y.; Kim, J.; Nam, W. *J. Am. Chem. Soc.* **2006**, *128*, 2630.
- (40) Mann, C. K.; Barnes, K. K. In *Electrochemical Reactions in Non-aqueous Systems*; Marcel Dekker: New York, 1970.
- (41) Thioanisoles can be protonated in the presence of a large excess of HClO₄ (see Figure S3 in the Supporting Information). The plots of k_1 vs concentration exhibit a saturation behavior in the region of high concentrations of thioanisoles due to the protonation of thioanisoles. Under the present experimental conditions in Figure S2 of the Supporting Information, the effect of the protonation of thioanisoles can be neglected.
- (42) (a) Fukuzumi, S.; Chiba, M.; Ishikawa, M.; Ishikawa, K.; Tanaka, T. *J. Chem. Soc., Perkin Trans. 2* **1989**, 1417. (b) Fukuzumi, S.; Ishikawa, M.; Tanaka, T. *Tetrahedron* **1986**, *42*, 1021. (c) Fukuzumi, S.; Chiba, M.; Tanaka, T. *Chem. Lett.* **1989**, 31.
- (43) The observed g_{\perp} value (2.58) is in good agreement with the value reported for [Ru^{III}(bpy)₃]³⁺, in which the g_{\parallel} component was not observed because of its weak intensity; see: (a) Matsuura, K.; Kevan, L. *J. Chem. Soc., Faraday Trans.* **1997**, *93*, 1763. (b) Kotani, H.;

Suenobu, T.; Lee, Y.-M.; Nam, W.; Fukuzumi, S. *J. Am. Chem. Soc.* **2011**, *133*, 3249.

(44) For similar Nernst analysis, see: (a) Yuasa, J.; Suenobu, T.; Fukuzumi, S. *J. Am. Chem. Soc.* **2003**, *125*, 12090. (b) Okamoto, K.; Imahori, H.; Fukuzumi, S. *J. Am. Chem. Soc.* **2003**, *125*, 7014.

(45) Goto, Y.; Matsui, T.; Ozaki, S.; Watanabe, Y.; Fukuzumi, S. *J. Am. Chem. Soc.* **1999**, *121*, 9497.

(46) Fukuzumi, S.; Nakanishi, I.; Tanaka, K.; Suenobu, T.; Tabard, A.; Guillard, R.; Caemelbecke, E.; Kadish, K. M. *J. Am. Chem. Soc.* **1999**, *121*, 785.

(47) For the difference between the inner-sphere and outer-sphere electron-transfer pathways, see: (a) Fukuzumi, S.; Wong, C. L.; Kochi, J. K. *J. Am. Chem. Soc.* **1980**, *102*, 2928–2939. (b) Fukuzumi, S.; Kochi, J. K. *Bull. Chem. Soc. Jpn.* **1983**, *56*, 969–979.

(48) (a) Fukuzumi, S.; Kochi, J. K. *J. Am. Chem. Soc.* **1981**, *103*, 2783.

(b) Fukuzumi, S.; Kochi, J. K. *J. Am. Chem. Soc.* **1981**, *103*, 7240.

(c) Fukuzumi, S.; Kochi, J. K. *J. Am. Chem. Soc.* **1982**, *104*, 7599.

(49) Rosokha, S. V.; Kochi, J. K. *Acc. Chem. Res.* **2008**, *41*, 641.

(50) For the classical definition of inner-sphere electron transfer, see: (a) Taube, H.; Myers, H. J.; Rich, R. L. *J. Am. Chem. Soc.* **1953**, *75*, 4118. (b) Taube, H. *Science* **1984**, *226*, 1028.